

Supporting information for

Flexible 3D Ordered SERS Sensor for Rapid and Reliable Detection of Pesticide Residues in Fruits

*Han Lu,^{a,b} Guangfei Huang,^c Dan Wang,^d Qilin Ma,^e Yuan Zhang,^c Mingliang Jin,^{*c,f} Lingling Shui^{*b,c}*

^a Institute of Carbon Neutrality, Zhejiang Wanli University, Ningbo 315100, China.

^b Guangdong Provincial Key Laboratory of Nanophotonic Functional Materials and Devices, School of Information and Optoelectronic Science and Engineering, South China Normal University, Guangzhou 510006, China. Email: shuill@m.scnu.edu.cn

^c International Joint Lab of Optofluidic Technology and System, National Center for International Research on Green Optoelectronics, South China Normal University, Guangzhou 510006, China. Email: jinml@scnu.edu.cn

^d Analysis & Testing Center, South China Normal University, Guangzhou 510006, China.

^e School of Electrical and Photoelectronic Engineering, West Anhui University, Luan 237012, China.

^f South China Academy of Advanced Optoelectronics, South China Normal University, Guangzhou 510006, China.

1. Experimental section

1.1. Materials

Hexadecyltrimethylammonium bromide (CTAB) and silver nitrate (AgNO_3) were obtained from Sigma-Aldrich (St. Louis, MO, USA). Hydrofluoric acid (HF, 49 wt%) was acquired from Aladdin (Shanghai, China). Rhodamine 6G (R6G) was supplied from J&K Chemical (Beijing, China). Methyl parathion solution (MPT, $\text{C}_8\text{H}_{10}\text{NO}_5\text{PS}$, 100 $\mu\text{g}/\text{mL}$ in methanol) was obtained from Sinopharm Chemical Reagent Co., Ltd. (Shanghai, China). Analytical grade hydrogen peroxide (H_2O_2 , 30 wt%), methanol, ethanol and sodium hydroxide (NaOH) were of analytical grade and sourced from Guangzhou Chemical Reagent Factory (Guangzhou, China). P-type (100) 4" Si wafers were purchased from Lijing Optoelectronics Co., Ltd. (Suzhou, China), and polystyrene (PS) nanospheres of 500 nm in diameter were acquired from Huge Bio-Chemical CO., Ltd. (Shanghai, China). Deionized (DI) water with a resistivity of 18.25 $\text{M}\Omega\cdot\text{cm}$ was obtained using a Milli-Q Plus water purification system (Milli-Q Plus water purification, Sichuan Wortel Water Treatment Equipment Co., Ltd., Sichuan, China). All chemicals used in the experiments were without any further purification.

To prepare the CTAB aqueous solution, CTAB was dissolved in DI water, and sonicated for 10 min at 40 °C. A stock solution of R6G with a concentration of 10^{-4} M was prepared by dissolving R6G powder in DI water, and then diluted to the required concentrations using DI water. The stock MPT solution was diluted to the desired concentrations by methanol.

1.2. Fabrication of SiNW arrays

The Si wafers were subjected to ultrasonic cleaning in DI water for 5 min, followed by immersing in Piranha solution for 30 min, and then thoroughly rinsed by DI water and dried with nitrogen gun. Nanosphere lithography was performed to pattern the SiNWs.¹ Briefly, the clean Si wafers were treated with O₂ plasma (MARCH AP-600, Nordson, USA) for 15 min to ensure a hydrophilic surface at the O₂ flow rate of 72 sccm, the pressure of 200 mTorr, and the radio frequency power of 500 W. Then, PS nanoparticles with diameter of 500 nm were self-assembled to form a monolayer on the cleaned Si wafer. Ar plasma etching was conducted in a plasma system to reduce the diameter of PS by controlling the etching time. The Ar flow rate was set to 72 sccm, the chamber pressure was 200 mTorr, and radio frequency power was 500 W. Afterwards, a 20 nm thick layer of Ag was deposited using magnetron sputtering (Q150T, Quorum Technologies Ltd, Ashford, Kent, England). After removing the PS in ethanol, metal-assisted chemical etching (MACE) was performed to form SiNW arrays by placing the patterned substrate into a mixed etchant containing 8.75 M HF and 1.32 M H₂O₂ at 20 °C for 5 min.

1.3. Fabrication of SiNW arrays with horizontal crack

SiNW arrays with horizontal crack were prepared following a previously reported method.² Briefly, the as-prepared SiNW arrays were subjected to thermal treatment in air at 200 °C for 180 min. Subsequently, the Si substrate was reimmersed in the etchant containing 8.75 M HF and 1.32 M H₂O₂ at 20 °C for the second MACE. Eventually, a horizontal crack would be formed after a given etching time.

1.4. Fabrication of SiNW@AgNP arrays

To decorate AgNPs onto the SiNWs surface, the SiNW arrays were then immersed in a mixture of 0.75 M HF, 0.03 M AgNO₃ and 4.5×10⁻² M CTAB at 20 °C for 5 min.³ After the reaction process, the sample was promptly transferred to a beaker filled with DI water and thoroughly rinsed by DI water to halt the reaction. After air drying at room temperature, SiNW@AgNP arrays were obtained.

1.5. Fabrication of flexible SiNW@AgNP arrays SERS substrates

In a typical procedure, the adhesive tape was applied on the top of SiNW@AgNP arrays with horizontal crack. The tape was subjected to uniform stress and firmly adhered to the SiNW@AgNP arrays. Subsequently, the SiNW@AgNP arrays were peeled off from the Si substrate using the tape.

1.6. SERS performance of flexible SiNW@AgNP arrays SERS substrates

As-prepared flexible SiNW@AgNP substrate was cut into pieces with a size of 0.5×0.5 cm² and immersed in 3.0 mL solutions containing probe molecules for SERS measurements. The SERS experiment employed a plastic cell with a diameter of 3.0 cm to contain the solution containing the probe molecules for SERS measurements. Raman spectra were measured by focusing on the SERS substrate in a solution using a Raman instrument (Finder Insight, Zolix Instruments Co., Ltd., Beijing, China) with the 532 nm laser line excitation. A 50× objective (NA = 0.55) was used to focus the laser beam onto the sample, producing a laser spot diameter of 10 μm. The incident power at the sample was set at 0.6 mW and the acquisition time of 0.1 s was used. Prior to each measurement, the SERS substrate was characterized in 3.0 mL DI water

as a reference. To evaluate the stability and reproducibility of the SERS substrates, a minimum of 5 different SERS substrates were prepared for each experiment, with 30 different points on each substrate selected to detect the probe molecules.

1.7. SERS detection of pesticide residues on apple peels

The apples were thoroughly rinsed with DI water prior to use. To ensure more reliable SERS detection, the apple peels were cut into $1.0 \times 1.0 \text{ cm}^2$ squares. Then, 10 μL of MPT solution with varying concentrations was spread onto the peel surface and dried at room temperature, respectively. Afterward, 10 μL of ethanol was dropped onto the pretreated apple peel in order to extract the MPT. The flexible SERS substrate was then pressed onto the apple peel for 10 s and peeled off slowly for further SERS analysis. The incident power at the sample was set at 0.6 mW and the acquisition time was 0.1 s.

1.8. Other characterization

The morphologies of SiNW@AgNP arrays were investigated using field emission-scanning electron microscopy (FE-SEM) (ZEISS-Ultra55, Carl Zeiss AG, Oberkochen, Germany). Chemical composition was analyzed using an energy dispersive spectroscope (EDS) equipped in FE-SEM.

The electric field distribution of the SiNW@AgNP arrays was simulated using finite-difference time-domain (FDTD) method. The simulation was conducted with an incident wavelength of 532 nm, oriented with the polarization direction along the x-axis. Mesh enclosing of the entire model was set to 1 nm per grid. Periodic boundary conditions were set in x-axis and y-axis, and perfectly matched layer in z-axis.

2. High-resolution SEM image of flexible SERS sensor

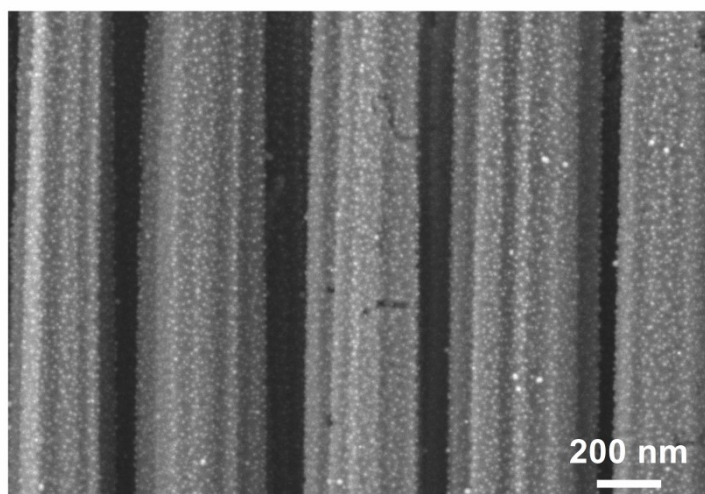


Fig. S1 High-resolution SEM image of as-prepared flexible SiNW@AgNP arrays.

3. Raman spectra of R6G

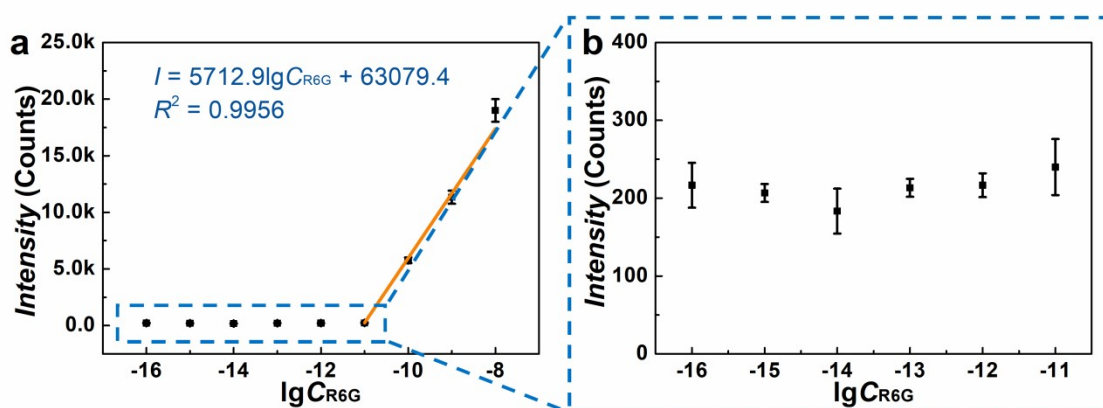


Fig. S2 (a) Raman intensity at 1650 cm^{-1} versus C_{R6G} in the range of 10^{-8} to 10^{-16} M.

(b) Raman intensity at 1650 cm^{-1} versus C_{R6G} in the range of 10^{-11} to 10^{-16} M.

4. Calculation of probe molecules

The corresponding probe molecules in different situations were calculated using the following formula.

$$N_{total} = C_{analytes} V_{total} N_A \quad (S1)$$

$$N_{laser\ min} = \frac{V_{laser}}{V_{total}} N_{total} \quad (S2)$$

$$N_{laser\ max} = \frac{S_{laser}}{S_{substrate}} N_{total} \quad (S3)$$

N_{total} is the total number of probe molecules located in the test cell. N_{laser} is the corresponding number of probe molecules located in the laser spots for Raman measurement. N_{laser} was estimated by two extreme cases. If probe molecules were uniformly distributed in the solution; therefore, only those molecules inside the laser column could possibly reside on the SERS substrate with $N_{laser\ min}$ being obtained. V_{total} is the total R6G volume located in the test cell, which was 3.0 mL. V_{laser} is the volume of the column of the laser spot, which was $3.3 \times 10^5 \mu\text{m}^3$. If probe molecules were all uniformly absorbed only on the SERS substrate surface, $N_{laser\ max}$ inside the laser spot area was achieved. S_{laser} is the area irradiated by the laser, which was $78.5 \mu\text{m}^2$. $S_{substrate}$ is the surface area of the SERS substrate, which was 0.25 cm^2 . $C_{analytes}$ is the corresponding concentration of used probe molecules in aqueous solutions for Raman measurement. N_A is Avogadro's constant. The corresponding probe molecules located in the test cell (N_{Total}) and in the laser spots for Raman measurements (N_{Laser}) at concentrations in the range of 10^{-8} - 10^{-16} M, as listed in **Table S2**.

5. Calculation of EF for R6G

The enhancement factor (EF) of R6G was calculated by applying the following equation,

$$EF = (I_{SERS}/N_{SERS})/(I_{bulk}/N_{bulk}) \quad (S4)$$

Where I_{SERS} and I_{bulk} are the Raman intensities of 10^{-16} M R6G on the flexible SiNW@AgNP arrays substrate and pure bulk R6G on the Si substrate at 1650 cm^{-1} , respectively (**Fig. S3**). N_{SERS} and N_{bulk} are the corresponding number of R6G molecules that contribute to the Raman intensities, respectively.

N_{bulk} was determined by assuming that the laser excitation volume has a cylinder shape with the circular diameter being equal to the focused laser spot diameter and the effective probe depth. Taking the diameter of the laser spot as $\sim 10 \text{ }\mu\text{m}$ and its permeation depth as $\sim 26 \text{ }\mu\text{m}$, the volume of R6G contributed to the pure bulk Raman signal inside the illuminated volume was $\sim 2041 \text{ }\mu\text{m}^3$. As a result, N_{bulk} is estimated $\sim 3.0 \times 10^{12}$ with the density of R6G 1.1702 g cm^{-3} . The Raman intensity (I_{bulk}) at 1650 cm^{-1} was calculated to ~ 650 . N_{SERS} was calculated based on two extreme cases with N_{laser} (minimum) and N_{laser} (maximum), corresponding N_{SERS} is $\sim 2.0 \times 10^{-2}$ and ~ 0.565 , respectively. The Raman intensity (I_{SERS}) at 1650 cm^{-1} was calculated to ~ 200 . The EFs for R6G at 1650 cm^{-1} were calculated to be 4.6×10^{13} and 1.7×10^{12} for the two extreme cases, respectively.

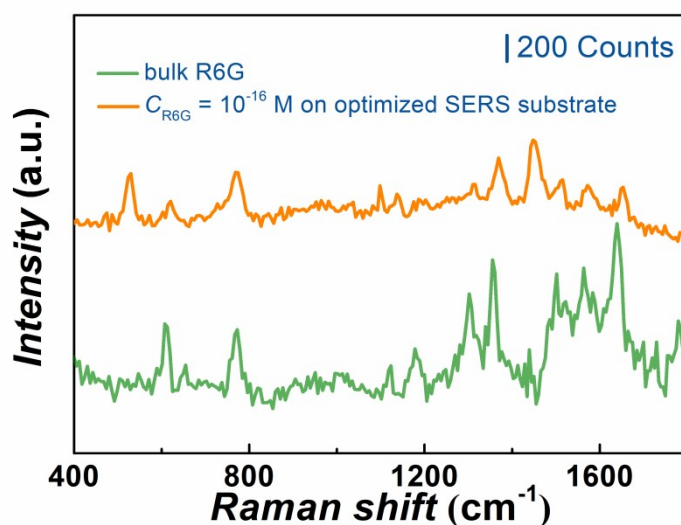


Fig. S3 Raman spectra of bulk R6G on Si substrate and 10^{-16} M R6G on the optimized flexible SERS substrate.

6. FDTD simulation

To further investigate the mechanism of SERS enhancement of the SiNW@AgNP arrays, the electric field distribution was simulated using FDTD method. Based on the SEM images, the AgNPs diameter was set as 20 nm, and SiNW arrays were set as with a length of 1 μm , a diameter of 320 nm, and a period of 500 nm. The incident wavelength was 532 nm, with the polarization direction along the x-axis. Mesh enclosing of the entire model was set to 1 nm per grid. Periodic boundary conditions were set in x-axis and y-axis, and perfectly matched layer in z-axis. As presented in **Fig. S4**, the maximum factor of 4 represents \log_{10} of a field enhancement $|E|^2$, which corresponds to an EF of 10^8 . Considering the chemical enhancement of $\sim 10^2$ - 10^4 , the total EF of $\sim 10^{10}$ - 10^{12} can be achieved, which is consistent with the experimental results.

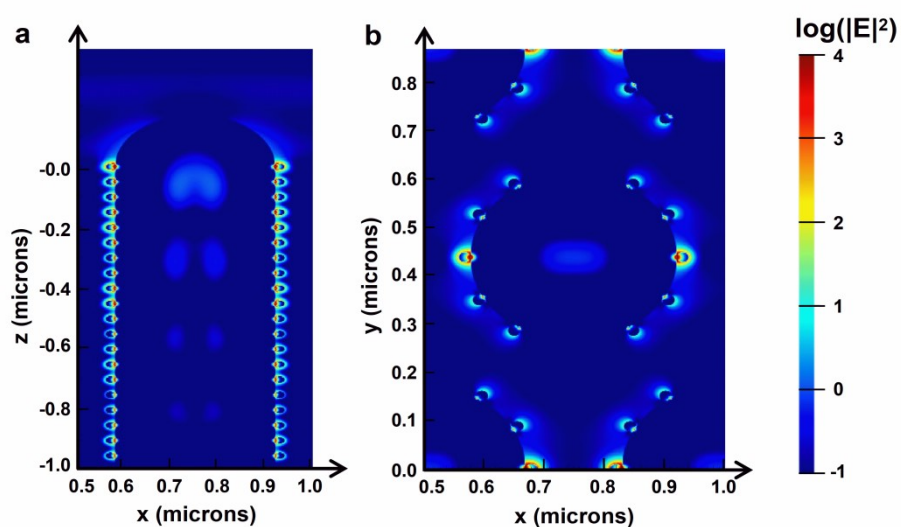


Fig. S4 FDTD simulation of the electric field distribution of SiNW@AgNP arrays. (a) side view, (b) top view. The scale bar is the log 10 of the a field enhancement $|E|^2$.

7. Reproducibility of as-prepared flexible SERS sensor

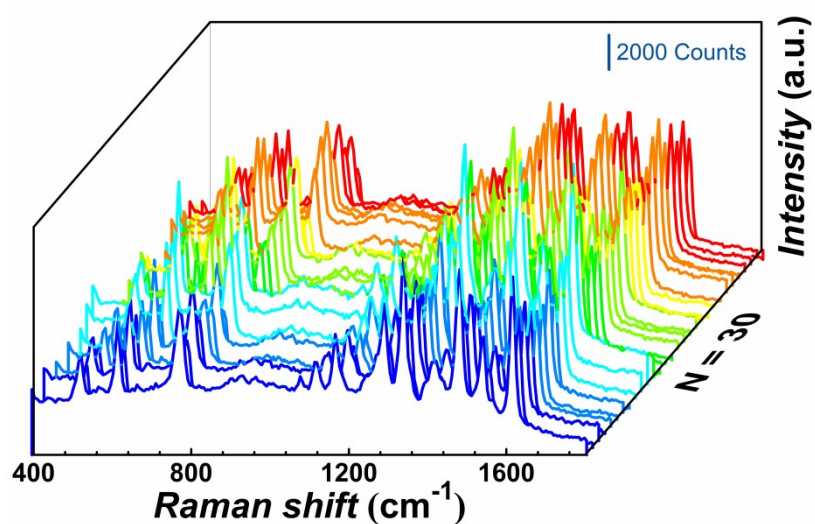


Fig. S5 30 Raman spectra of 10^{-10} M R6G measured by randomly moving one sample SERS substrate.

8. Bending tests of flexible SiNW@AgNP arrays SERS sensor

The bending test was evaluated for the mechanical robustness of flexible SERS sensor over 100 cycles. For bending test, the flexible SERS sensor was bent in half. The SEM images and Raman spectra of flexible SiNW@AgNP arrays SERS sensor before and after 100 cycles of bending were presented in **Fig. S6**, indicating that the flexible SERS sensor showed acceptable mechanical stability.

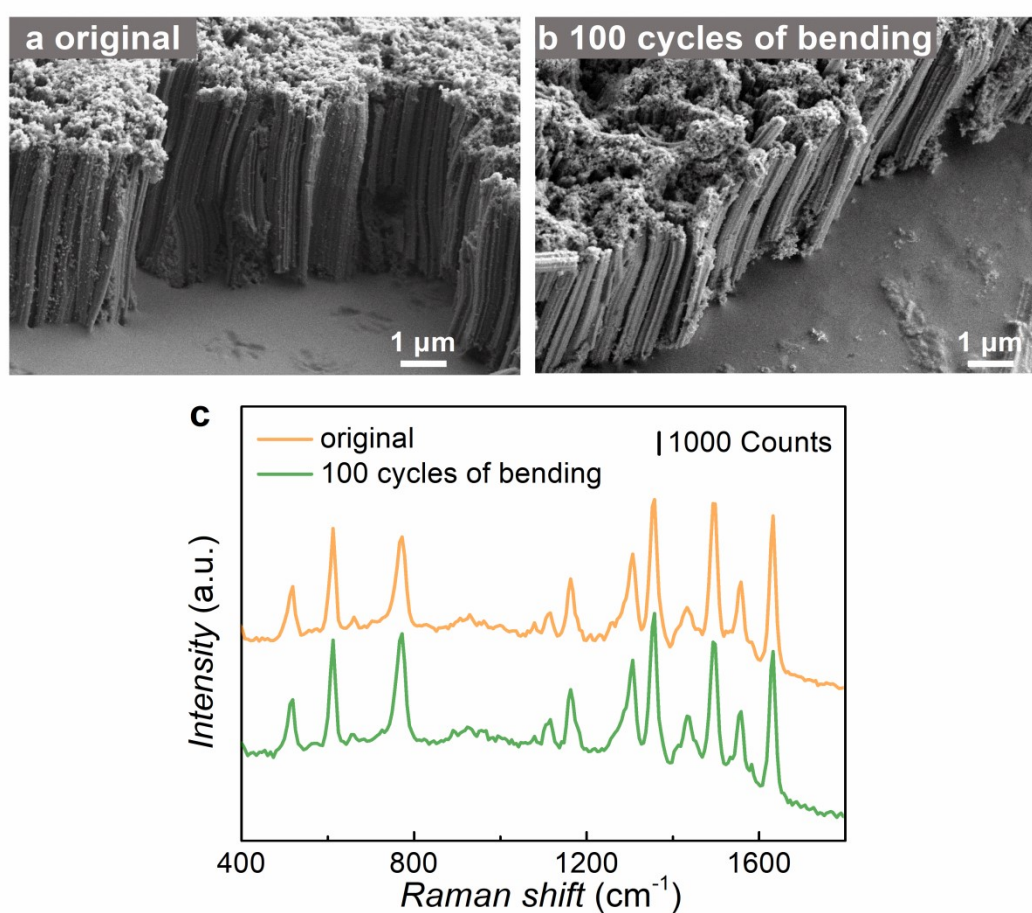


Fig. S6. SEM images of flexible SERS sensor (a) before and (b) after 100 cycles of bending. (c) Raman spectra of 10^{-10} M R6G collected on the flexible SERS sensor before and after 100 cycles of bending.

9. Reproducibility of as-prepared flexible SERS sensor

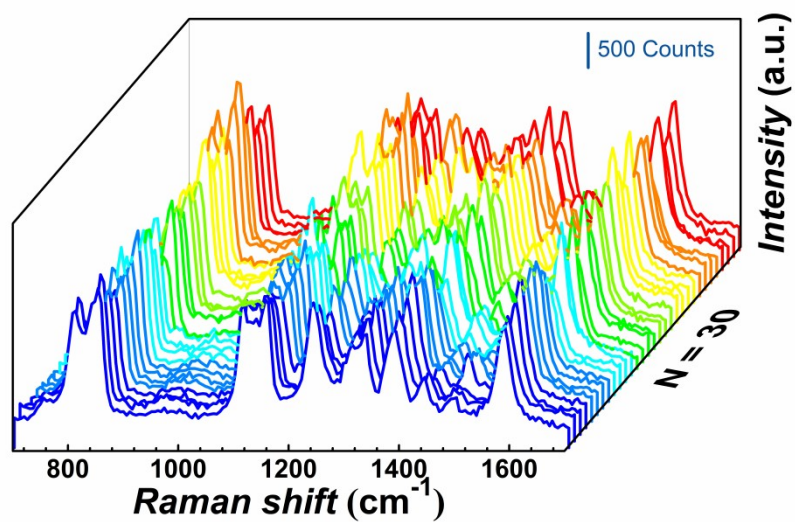


Fig. S7. 30 Raman spectra of 10^{-6} M MPT measured by randomly moving one sample SERS substrate.

Table S1 Raman peaks and corresponding vibration modes of R6G.^{4, 5}

Raman shift (cm ⁻¹)	Vibration mode
612	C-C-C ring in-plane bending
771	C-H out-of-plane bending
1125	C-H in-plane bending
1189	symmetric modes of C-C stretching vibration
1310	C-O-C in-plane bending
1360	symmetric modes of C-C stretching vibration
1510	symmetric modes of C-C stretching vibration
1573	symmetric modes of C-C stretching vibration
1650	symmetric modes of C-C stretching vibration

Table S2 Calculation of probe molecules in the test cell and laser spot.

C_{analytes}/M	10^{-16}	10^{-15}	10^{-14}	10^{-13}	10^{-12}	10^{-11}	10^{-10}	10^{-9}	10^{-8}
N_{total}	1.8×10^5	1.8×10^6	1.8×10^7	1.8×10^8	1.8×10^9	1.8×10^{10}	1.8×10^{11}	1.8×10^{12}	1.8×10^{13}
$N_{\text{laser min}}$	2.0×10^{-2}	0.2	2.0	20.0	2.0×10^2	2.0×10^3	2.0×10^4	2.0×10^5	2.0×10^6
$N_{\text{laser max}}$	5.65×10^{-1}	5.65	56.5	5.65×10^2	5.65×10^3	5.65×10^4	5.65×10^5	5.65×10^6	5.65×10^7

Table S3 Raman peaks and corresponding vibration modes of MPT.^{6,7}

Raman shift (cm ⁻¹)	Vibration mode
849	P-O stretch
1152	C-N stretch
1341	C-O stretch
1586	phenyl stretch

Table S4 Comparison of the reported flexible SERS sensors for MPT residue determination.

SERS sensors	LOD	Reference
AgNP@PDMS arrays	2.5×10^{-8} g/cm ²	8
Au NPs on tape	2.6×10^{-9} g/cm ²	9
PDADMAC/PSS/Au@Ag NRs filter paper	7.2×10^{-11} g/cm ²	10
bipyramid-AuNPs on tape	3.7×10^{-11} g/cm ²	11
Au NPs on paper	1.1×10^{-8} g/cm ²	12
Ag/Au NWs/PDMS film	3.8×10^{-9} M	13
g-C ₃ N ₄ @MoS ₂ @Ag	4.8×10^{-6} mg/mL	14
Ag NWs@ZIF-8 core-shell nanochains	7.6×10^{-9} M	15
Au@Ag NRs	3.7×10^{-11} g/cm ²	16
Rose-petal-like substrate	1.2×10^{-9} g/cm ²	17
AgNP@SiNW arrays	10^{-9} M (2.6×10^{-12} g/cm ²)	This work

References

1. J. A. Huang, Y. Q. Zhao, X. J. Zhang, L. F. He, T. L. Wong, Y. S. Chui, W. J. Zhang and S. T. Lee, *Nano Lett.*, 2013, **13**, 5039-5045.
2. Y. Wang, X. Zhang, P. Gao, Z. Shao, X. Zhang, Y. Han and J. Jie, *ACS Appl. Mater. Interfaces*, 2014, **6**, 977-984.
3. H. Lu, M. Jin, Q. Ma, Z. Yan, Z. Liu, X. Wang, E. M. Akinoglu, A. van den Berg, G. Zhou and L. Shui, *Sensor. Actuat. B-Chem.*, 2020, **304**, 127224.
4. P. Ran, L. Jiang, X. Li, B. Li, P. Zuo and Y. Lu, *Small*, 2019, **15**, 1804899.
5. Y. Wang, M. Zhang, L. Feng, B. Dong, T. Xu, D. Li, L. Jiang and L. Chi, *Small*, 2019, **15**, 1804527.
6. P. Wang, L. Wu, Z. Lu, Q. Li, W. Yin, F. Ding and H. Han, *Anal. Chem.*, 2017, **89**, 2424-2431.
7. J. Chen, Y. Huang, P. Kannan, L. Zhang, Z. Lin, J. Zhang, T. Chen and L. Guo, *Anal. Chem.*, 2016, **88**, 2149-2155.
8. P. Wang, L. Wu, Z. Lu, Q. Li, W. Yin, F. Ding and H. Han, *Anal. Chem.*, 2017, **89**, 2424-2431.
9. J. Chen, Y. Huang, P. Kannan, L. Zhang, Z. Lin, J. Zhang, T. Chen and L. Guo, *Anal. Chem.*, 2016, **88**, 2149-2155.
10. Z. Chen, Y. Sun, J. Shi, W. Zhang, X. Zhang, X. Hang, Z. Li and X. Zou, *Food Chem.*, 2023, **424**, 136232.
11. H. Wu, Y. Luo, C. Hou, D. Huo, Y. Zhou, S. Zou, J. Zhao and Y. Lei, *Sensor. Actuat. B-Chem.*, 2019, **285**, 123-128.
12. J. Xie, L. Li, I. M. Khan, Z. Wang and X. Ma, *Spectrochim. Acta A*, 2020, **231**,

118104.

13. Y. Ma, Y. Du, Y. Chen, C. Gu, T. Jiang, G. Wei and J. Zhou, *Chem. Eng. J.*, 2020, **381**, 122710.
14. R. Wang, J. Ma, X. Dai, Y. Gao, C. Gu and T. Jiang, *Sensor. Actuat. B-Chem.*, 2023, **374**, 132782.
15. J. Yang, M. Pan, X. Yang, K. Liu, Y. Song and S. Wang, *Food Chem.*, 2022, **395**, 133623.
16. Z. Chen, Y. Sun, X. Zhang, Y. Shen, S. A. M. Khalifa, X. Huang, J. Shi, Z. Li and X. Zou, *Food Chem.*, 2024, **441**, 135087.
17. Y. Wang, C. Chen, J. Lu, J. Liu, J. Zhai, H. Zhao and N. Lu, *Sensor. Actuat. B-Chem.*, 2024, **402**, 138345.